

# STUDY OF $B_s^0 \rightarrow \mu^+ \mu^-$ IN CMS

URS LANGENEGGER\*

*Institute for Particle Physics, ETH Zurich, 8093 Zurich, Switzerland*

*\*E-mail: ursl@phys.ethz.ch*

We present a Monte Carlo simulation study of measuring the rare leptonic decay  $B_s^0 \rightarrow \mu^+ \mu^-$  with the CMS experiment at the LHC. The study is based on a full detector simulation for signal and background events. We discuss the high-level trigger algorithm and the offline event selection.

*Keywords:* Rare  $B$  decays; Supersymmetry; LHC

## 1. Introduction

In the standard model (SM), the decay  $B_s^0 \rightarrow \mu^+ \mu^-$  has a highly suppressed rate<sup>1</sup> of  $\mathcal{B} = (3.42 \pm 0.54) \times 10^{-9}$  since it involves a  $b \rightarrow s$  transition and requires an internal quark annihilation which further suppresses the decay relative to the electroweak ‘penguin’  $b \rightarrow s\gamma$  decay. In addition, the decays are helicity suppressed by factors of  $m_\ell^2$ . To date these decays have not been observed; upper limits on these branching fractions are a topic of frequent updates at the  $B$ -factories<sup>2,3</sup> (for the decay  $B_d^0 \rightarrow \mu^+ \mu^-$ ) and the Tevatron.<sup>4,5</sup> Currently the best upper limit is from the CDF collaboration<sup>5</sup> with  $\mathcal{B}(B_s^0 \rightarrow \mu^+ \mu^-) < 1.0 \times 10^{-7}$  at 95% confidence limit.

Since these processes are highly suppressed in the SM, they are potentially sensitive probes of physics beyond the SM (see Fig. 1). In the minimal supersymmetric extension of the SM (MSSM) the branching fraction for these decays can be substantially enhanced, especially at large  $\tan\beta$ .<sup>6</sup> For MSSM with modified minimal flavor violation at large  $\tan\beta$ , the branching fraction can be increased by up to four orders of magnitude.<sup>7</sup>  $B_{s(d)}^0 \rightarrow \mu^+ \mu^-$  decays can also be enhanced in specific models containing leptoquarks<sup>8</sup> and supersymmetric (SUSY) models without R-parity.<sup>9</sup>

There has been some interest<sup>10,11,12</sup> in using the decay mode  $B_s^0 \rightarrow \mu^+ \mu^-$  to ‘mea-

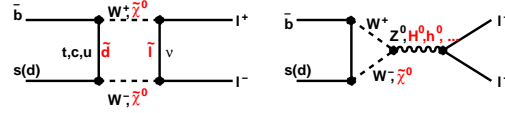


Fig. 1. Feynman graphs for the decay  $B_{s(d)}^0 \rightarrow \mu^+ \mu^-$  illustrating possible new physics contributions.

sure’ the key parameter  $\tan\beta$  of the MSSM and to constrain other extensions of the SM. Lower bounds on  $\tan\beta$  can be obtained from  $\mathcal{B}(B_s^0 \rightarrow \mu^+ \mu^-)$  with general model-independent assumptions. Since  $\tan\beta$  is also constrained from above due to general principles, a lower bound is tantamount to a measurement of  $\tan\beta$ .

## 2. The CMS Experiment

The Compact Muon Solenoid (CMS) detector is well suited for the study of leptonic  $B$  decays. The main components for this analysis are the tracker and muon systems.

The CMS tracker is an all-silicon detector, comprises an inner pixel vertex detector plus an outer strip track detector, and is immersed in a magnetic field of 4 T. The pixel detector provides high-precision measurements of space points close to the interaction region for vertexing and effective pattern recognition in the high-track multiplicity environment at the LHC. The pixel detector is composed of 1440 modules arranged in three barrel layers (at a radial distance of

$r = 4.4, 7.3, 10.2$  cm from the beampipe) and four endcap disks (at  $z = \pm 34.5, \pm 46.5$  cm from the interaction point). The barrel detector comprises 672 modules and 96 half-modules, the forward detector is built of 96 blades with 672 modules. With a pixel size of  $d_\phi \times d_z = 100 \mu\text{m} \times 150 \mu\text{m}$ , a hit resolution of  $10\text{--}20 \mu\text{m}$  is achieved. The strip tracker allows the precise determination of charged particle momenta. It is arranged in the central part as inner (TIB) and outer (TOB) barrel, and in the forward regions as inner discs (TID) and endcaps (TEC). The barrel part consists of 10 layers (4 in the TIB, 6 in the TOB) and 12 layers in the forward part (3 in the TID, 9 in the TEC). The pitch in the strip tracker varies between  $80\text{--}180 \mu\text{m}$ . The material inside the active volume of the tracker increases from  $\approx 0.4X_0$  at pseudorapidity  $\eta = 0$  to around  $1X_0$  at  $|\eta| \approx 1.6$ , before decreasing to  $\approx 0.6X_0$  at  $|\eta| = 2.5$ .

The CMS muon system, incorporated into the magnet return yoke, is divided into a barrel ( $|\eta| < 1.2$ ) and forward parts ( $1.2 < |\eta| < 2.4$ ). In the barrel region, where the neutron induced background and the muon rate is small, drift tube (DT) chambers are used. In the two endcaps cathode strip chambers (CSC) are deployed. In addition, resistive plate chambers (RPC) are used both in the barrel and the endcap region. The RPC spatial resolution is coarser than for the DT and CSC, but their excellent time resolution allows the unambiguous identification of the correct bunch crossing.

### 3. Event Samples

Monte Carlo (MC) event samples were generated with PYTHIA 6.227 and passed through a full detector simulation based on GEANT 4. On average five pile-up events were included, appropriate for a luminosity of  $\mathcal{L} = 2 \times 10^{33} \text{ cm}^{-2} \text{ s}^{-1}$ .

Both signal and background MC event samples have been generated as minimum

bias QCD events. In the signal sample,  $B_s$  mesons decay as  $B_s^0 \rightarrow \mu^+ \mu^-$ . The muons are required to have transverse momentum  $p_\perp^\mu > 3 \text{ GeV}$  and  $|\eta^\mu| < 2.4$ ; the  $B_s$  must have  $p_\perp^{B_s} > 5 \text{ GeV}$ .

The background sample contains two muons with  $p_\perp > 3 \text{ GeV}$  and  $|\eta| < 2.4$ . Their separation in azimuth and pseudorapidity  $\Delta R(\mu\mu) \equiv \sqrt{\Delta\phi^2 + \Delta\eta^2}$  is required to be  $0.3 < \Delta R(\mu\mu) < 1.8$ . Currently the background simulation does not include muons due to hadronic in-flight decays or punch-through. It is estimated that this hadronic component will increase the background level by about 10%. Background events from rare  $B_d, B_u, B_s, B_c, \Lambda_b$  decays are not included.

In total 20000 signal events and about 15000 background events have been analyzed. The small size of the background sample is the limiting factor of the present study.

### 4. Trigger Strategy

The CMS detector has a twofold trigger strategy. The first level trigger, with a latency of  $3.2 \mu\text{s}$ , is based on information from the calorimeters and the muon system. The threshold for inclusive isolated single muons is at  $p_\perp^\mu > 14 \text{ GeV}$ , for dimuon events both muons must have  $p_\perp > 3 \text{ GeV}$ . The expected trigger rates amount to  $2.7 \text{ kHz}$  and  $0.9 \text{ kHz}$ , respectively. The L1 trigger output rate is at most  $100 \text{ kHz}$ .

The high-level trigger (HLT) is a software trigger, running on a large processor farm. The HLT reduces the overall trigger rate by three orders of magnitude to about  $100 \text{ Hz}$ . To fit into the tight time constraints imposed by the high input rate, tracking at the HLT is sped up by two concepts: (1) ‘Regional seed generation’ limits track seeding to specific regions of interest, *e.g.*, a cone around the L1 muon candidate direction. (2) ‘Partial tracking’ pursues track reconstruction only until some criteria are met, *e.g.*, a resolution of 2% on the transverse momen-

tum. Already with six reconstructed hits, both the efficiency and the resolution are comparable to the full tracking performance.

The HLT strategy for  $B_s^0 \rightarrow \mu^+\mu^-$  proceeds along the following path. (1) Verification of the two L1 muon candidates. (2) Tracks reconstructed only with the pixel detector are used to compute a list of possible primary vertices, the three most significant are retained. (3) Regional track reconstruction with up to six hits is performed in cones around the L1 muon candidates. (4) Reconstructed tracks with  $p_\perp > 4$  GeV are paired and retained if their invariant mass falls into predefined regions for the signal and sidebands. (5) The two tracks must have opposite charge and are fit to a common vertex; the event is retained only when the fit  $\chi^2 < 20$  and the three-dimensional flight length  $l_{3d} > 150 \mu\text{m}$ . With this selection, the event rate was estimated<sup>13</sup> to be  $< 1.7$  Hz.

## 5. Offline Analysis

The offline analysis selection focuses on a secondary vertex that is well measured and separated from the primary vertex and consistent with the decay of an isolated  $B_s$  meson.

The primary vertex is determined from all tracks with  $p_\perp > 0.9$  GeV, because of the rather low-multiplicity track environment.

The two muons must have opposite charge,  $p_\perp^\mu > 4.0$ , and  $|\eta^\mu| < 2.4$ . The azimuthal and pseudorapidity separation of the two muons  $0.3 < \Delta R(\mu\mu) < 1.2$  provides a powerful reduction of gluon-gluon fusion background with both  $b$ -hadrons decaying semileptonically: The muons of those  $b$ -hadrons tend to be back-to-back, while the signal shows a peaked distribution with a maximum at  $\Delta R(\mu\mu) \sim 1$ .

$B_s$  candidates are formed by vertexing the two muon candidates. The vertex quality is required to be  $\chi^2 < 1.0$ . The transverse momentum vector of the  $B_s$  candidate must be close to the displacement of the secondary

vertex from the primary vertex: the cosine of the opening angle  $\alpha$  between the two vectors must fulfill  $\cos(\alpha) > 0.995$ . The significance of the  $B_s$  candidate flight length  $l_{xy}$  in the transverse plane is defined as  $l_{xy}/\sigma_{xy}$  (illustrated in Fig. 2), where  $\sigma_{xy}$  is the error on the flight length with mean  $\langle\sigma_{xy}\rangle = 120 \mu\text{m}$ ; we require  $l_{xy}/\sigma_{xy} > 18.0$ .

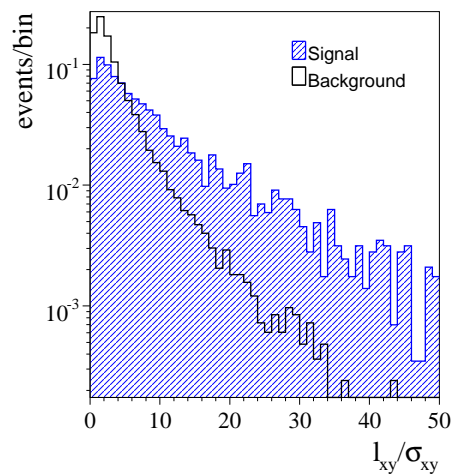


Fig. 2. Decay length significance in the transverse plane for signal and background MC events. Both histograms are normalized to unity.

In high- $p_\perp$  gluon-splitting events the  $b\bar{b}$  quark pair moves closely together due to their boost, and the two decay vertices of the resulting  $b$ -hadrons cannot be well separated in all cases. However, because of color reconnection, the hadronic activity around the dimuon direction is enhanced compared to the signal decay (where only one colorless  $B_s$  meson decays). This is exploited in isolation requirements: The isolation  $I$  is determined from the dimuon transverse momentum and charged tracks with  $p_\perp > 0.9$  GeV in a cone with half-radius  $r = 1.0$  around the dimuon direction as  $I \equiv p_\perp^{\mu\mu}/(p_\perp^{\mu\mu} + \sum_{trk} |p_\perp|)$ ; we require  $I > 0.85$ .

Figure 3 illustrates the mass resolution obtained on the signal MC event sample.

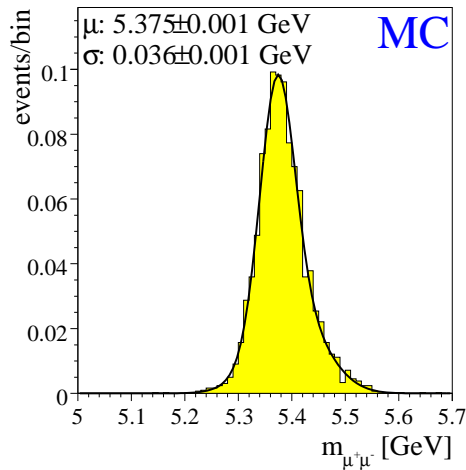


Fig. 3. Dimuon mass distribution in signal MC events. The curve is a fit of two Gaussians, the displayed parameters indicate the average mean and sigma. The histogram is normalized to unity.

The distribution is fit with two Gaussians, the quoted width  $\sigma = 36.0 \text{ MeV}$  is determined according to

$$\sigma^2 = \frac{N_n^2 \sigma_n^2 + N_w^2 \sigma_w^2}{N_n^2 + N_w^2},$$

where  $\sigma_n = 32.1 \text{ MeV}$  ( $\sigma_w = 60.2 \text{ MeV}$ ) and  $N_n = 0.08$  ( $N_w = 0.03$ ) are the width and normalization of the narrow (wide) Gaussian, respectively.

Given the limited statistics of the background sample, no event remains after the application of all selection requirements. However, the absence of correlation to the other selection requirements allows a factorization of the isolation and  $\chi^2$  requirements from the other cuts in the determination of the total background rejection factor. The dominant sources of uncertainty on the signal ( $\pm 25\%$ ) and background ( $^{+160}_{-100}\%$ ) yield are the statistical component of the background sample, the impact of the misalignment on the transverse flight length significance, and the assumption of factorizing cuts.

The total selection efficiency for signal events is  $\varepsilon_S = 0.019 \pm 0.002$  and the back-

ground reduction factor is  $\varepsilon_B = 2.74 \times 10^{-7}$ . With this selection, the first  $10.0 \text{ fb}^{-1}$  of integrated luminosity will yield  $n_S = 6.1 \pm 0.6$  signal events and  $n_B = 13.8^{+22.0}_{-13.8}$  background events in a mass window of  $m_{B_s} \pm 0.1 \text{ GeV}$ . With this background estimate, the upper limit on the branching fraction is  $\mathcal{B}(B_s^0 \rightarrow \mu^+ \mu^-) \leq 1.4 \times 10^{-8}$  at the 90% C.L.

## 6. Conclusions

This study is limited by the size of the background MC sample. In the future, it will include larger background samples and a detailed simulation of rare  $b$ -hadron decays. The search for  $B_s^0 \rightarrow \mu^+ \mu^-$  promises an interesting start-up analysis with the possibility of setting tight constraints on the MSSM. With sufficient integrated luminosity, the precision measurement of the  $B_s^0 \rightarrow \mu^+ \mu^-$  branching fraction will set constraints on models of new physics.

## References

1. A. J. Buras, Phys. Lett. B **566**, 115 (2003).
2. M. C. Chang *et al.* [BELLE Collaboration], Phys. Rev. D **68**, 111101 (2003).
3. B. Aubert *et al.* [BABAR Collaboration], Phys. Rev. Lett. **94**, 221803 (2005).
4. V. M. Abazov *et al.* [D0 Collaboration], Phys. Rev. Lett. **94**, 071802 (2005).
5. A. Abulencia *et al.* [CDF collaboration], CDF Public Note 8176 (2006).
6. K. S. Babu and C. F. Kolda, Phys. Rev. Lett. **84**, 228 (2000); S. R. Choudhury and N. Gaur, Phys. Lett. B **451**, 86 (1999); C. S. Huang, *et al.*, Phys. Rev. D **63**, 114021 (2001).
7. C. Bobeth, T. Ewerth, F. Kruger and J. Urban, Phys. Rev. D **66**, 074021 (2002).
8. S. Davidson, D. C. Bailey and B. A. Campbell, Z. Phys. C **61**, 613 (1994).
9. D. P. Roy, Phys. Lett. B **283**, 270 (1992).
10. G. L. Kane, C. Kolda and J. E. Lennon, arXiv:hep-ph/0310042.
11. S. Baek, Phys. Lett. B **595**, 461 (2004).
12. A. Dedes and B. T. Huffman, Phys. Lett. B **600**, 261 (2004).
13. P. Sphicas *et al.* [CMS Collaboration], CERN-LHCC-2002-026.